

**ESI**

**For**

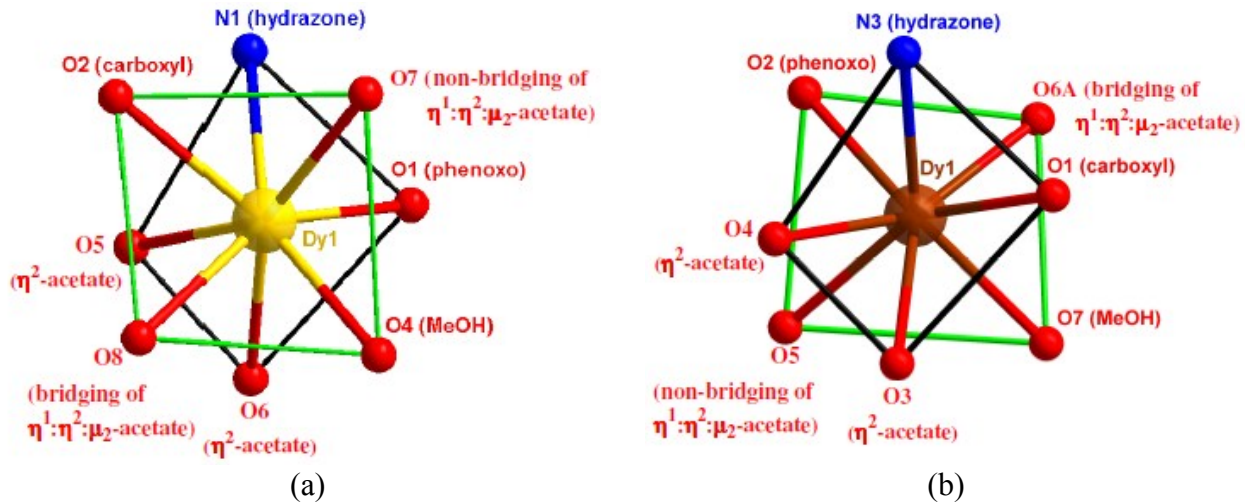
**Experimental and Theoretical exploration of magnetic exchange interactions  
and single molecule magnetic behaviour of bis( $\eta^1:\eta^2:\mu_2$ -carboxylate)  
 $\text{Gd}^{\text{III}}_2/\text{Dy}^{\text{III}}_2$  systems**

**Sagar Ghosh,<sup>a</sup> Shuvankar Mandal,<sup>a</sup> Mukesh Kumar Singh,<sup>b</sup> Cai-Ming Liu,<sup>c</sup> Gopalan Rajaraman<sup>\*b</sup> and Sasankasekhar Mohanta<sup>\*a</sup>**

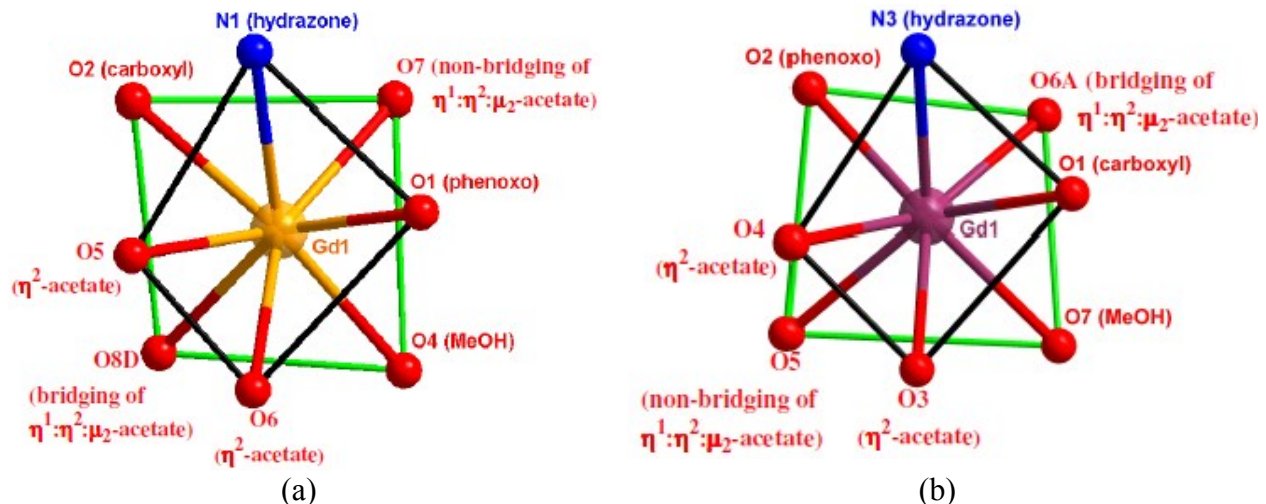
<sup>a</sup>*Department of Chemistry, University of Calcutta, 92 A. P. C. Road, Kolkata 700 009, India,  
Fax: 91-33-23519755, E-mail: sm\_cu\_chem@yahoo.co.in.*

<sup>b</sup>*Department of Chemistry, Indian Institute of Technology Bombay, Powai, Mumbai 400076,  
India. Email: rajaraman@chem.iitb.ac.in.*

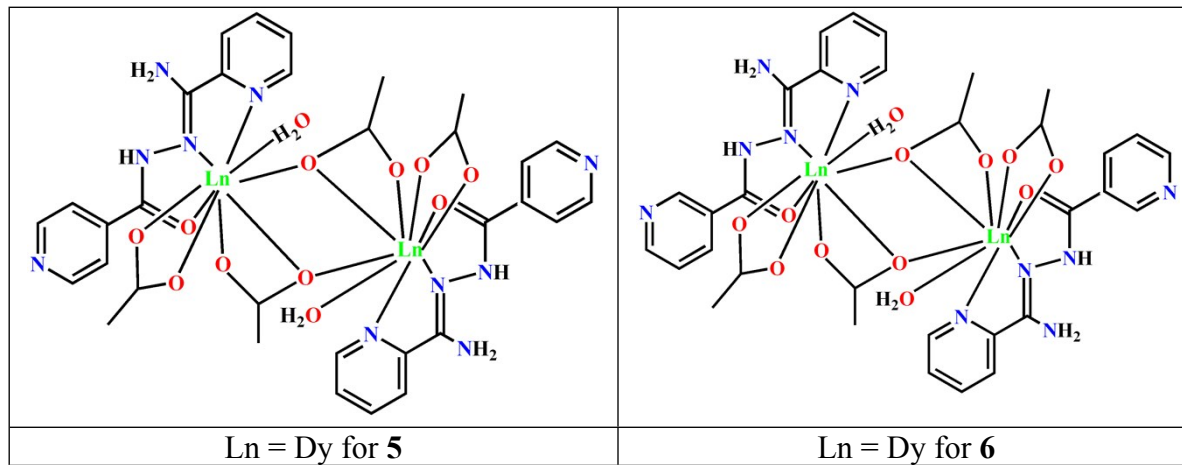
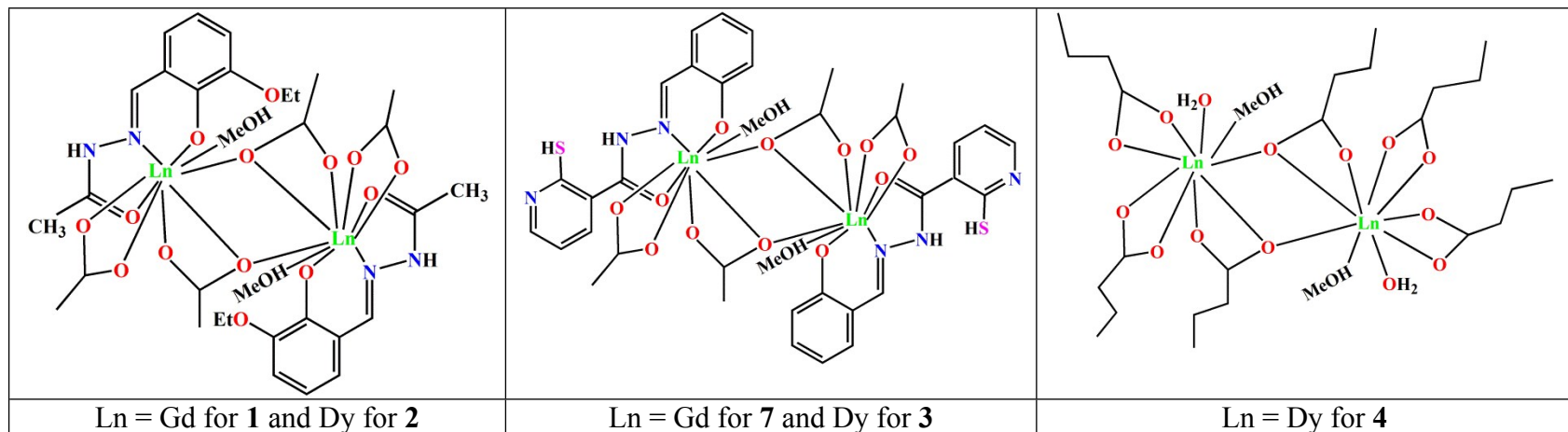
<sup>c</sup>*Beijing National Laboratory for Molecular Sciences, Center for Molecular Science, Institute of  
Chemistry, Chinese Academy of Sciences, Beijing 100190, PR China.*



**Scheme S1.** Comparative coordination environment in  $[Dy^{III}L_2(\text{acetate})_4(\text{MeOH})_2]$  (**2**) and  $[Dy^{III}L_1^2(\text{acetate})_4(\text{MeOH})_2] \cdot 2\text{MeOH}$  (**3**) shown as (a) and (b), respectively. The capped oxygen atom (the bridging O atom of one  $\eta^1:\eta^2:\mu_2$ acetate in both) is not shown for clarity.



**Scheme S2.** Comparative coordination environment in  $[Gd^{III}L_2(\text{acetate})_4(\text{MeOH})_2]$  (**1**) and  $[Gd^{III}L_1^2(\text{acetate})_4(\text{MeOH})_2] \cdot 2\text{MeOH}$  (**7**) shown as (a) and (b), respectively. The capped oxygen atom (the bridging O atom of one  $\eta^1:\eta^2:\mu_2$ acetate in both) is not shown for clarity.



**Scheme S3.** Chemical structures of **1**, **2** and related compounds **3–7**.

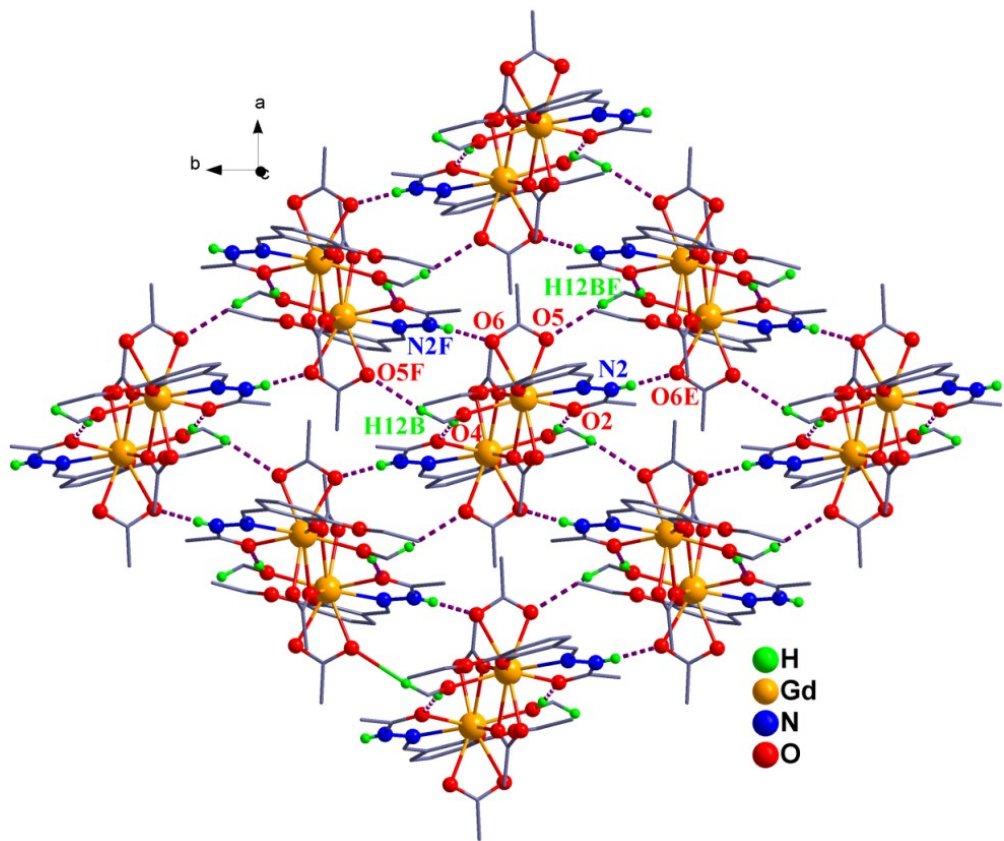


**Fig. S1.** Perspective view of the two-dimensional sheet in the crystallographic *ab* plane of  $[\text{Gd}_2\text{L}_2(\text{OAc})_4(\text{MeOH})_2]$  (**1**). Only the hydrogen atoms participating in hydrogen bonding interactions are shown. Symmetry Code: E,  $1.5-x, -0.5+y, 1.5-z$ ; F,  $1.5-x, 0.5+y, 1.5-z$ .

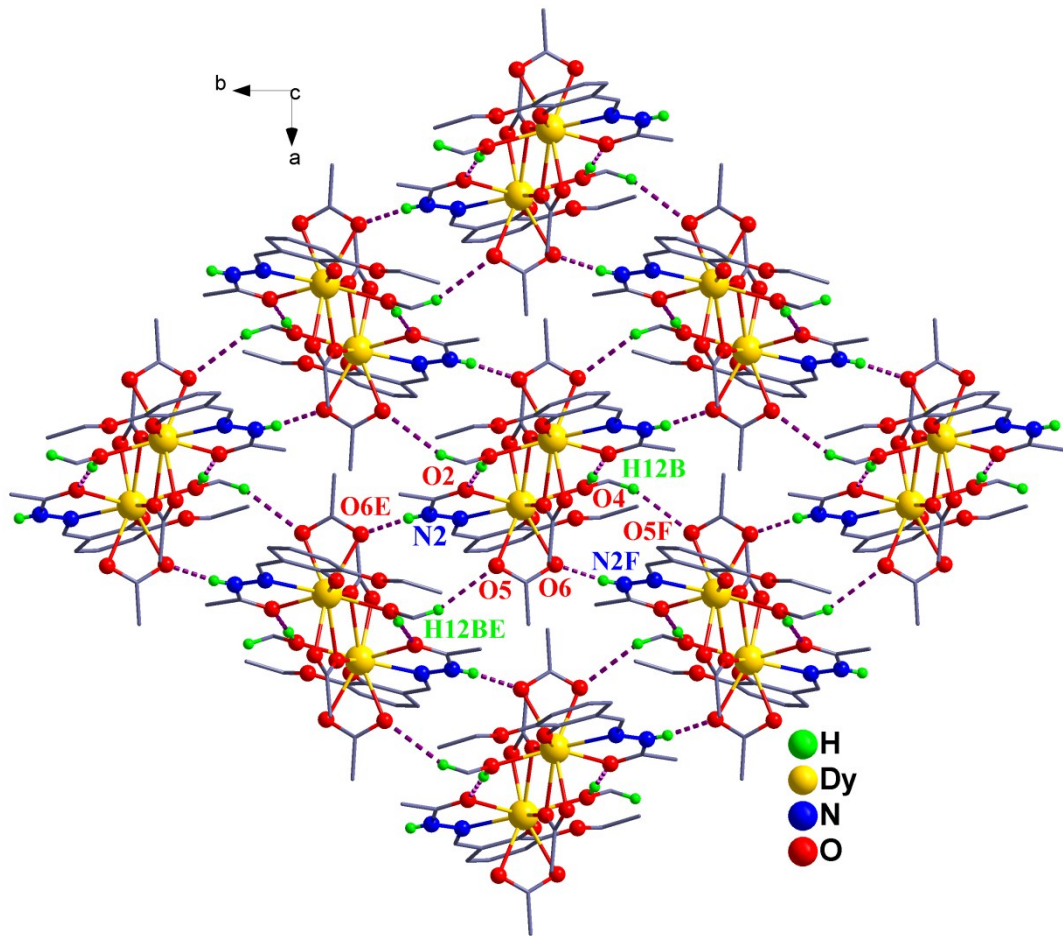


**Fig. S2.** Perspective view of the two-dimensional sheet in the crystallographic *ab* plane of  $[\text{Dy}_2\text{L}_2(\text{OAc})_4(\text{MeOH})_2]$  (**2**). Only the hydrogen atoms participating in hydrogen bonding interactions are shown. Symmetry Code: E,  $0.5-x$ ,  $0.5+y$ ,  $0.5-z$ ; F,  $0.5-x$ ,  $-0.5+y$ ,  $0.5-z$ .

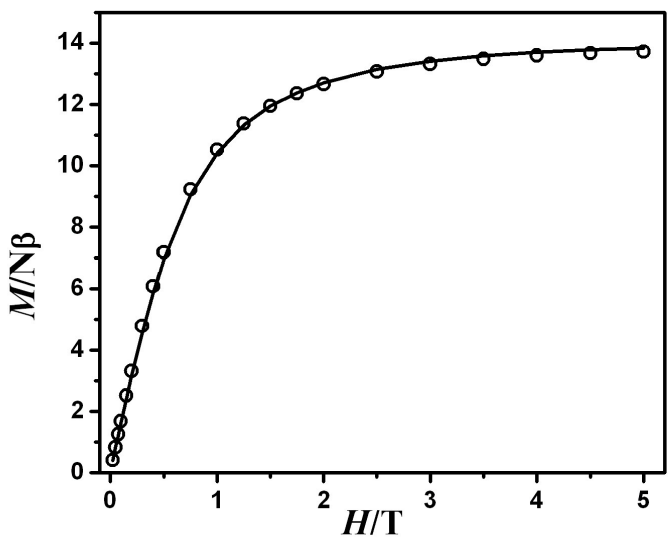


**Fig. S3.** Magnetization ( $M$ ) vs Field ( $H$ ) plots for  $[\text{Gd}_2\text{L}_2(\text{OAc})_4(\text{MeOH})_2]$  (**1**) at 2K. The solid line corresponds to the best fit using the *PHI* program.

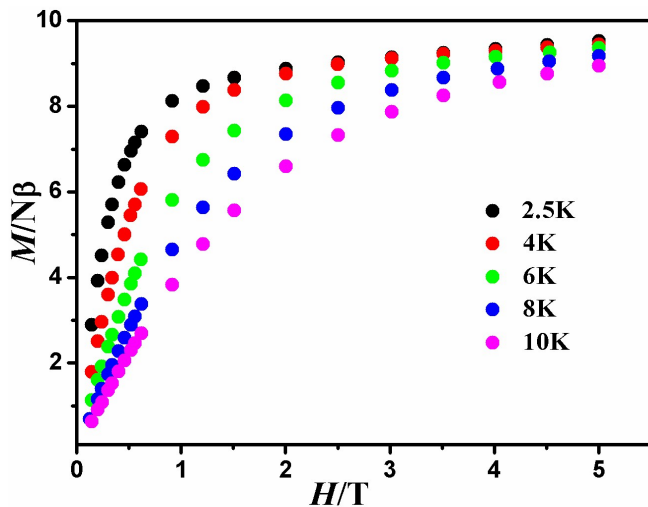


**Fig. S4.** Magnetization ( $M$ ) vs Field ( $H$ ) plots for  $[\text{Dy}_2\text{L}_2(\text{OAc})_4(\text{MeOH})_2]$  (**2**) at different temperatures.

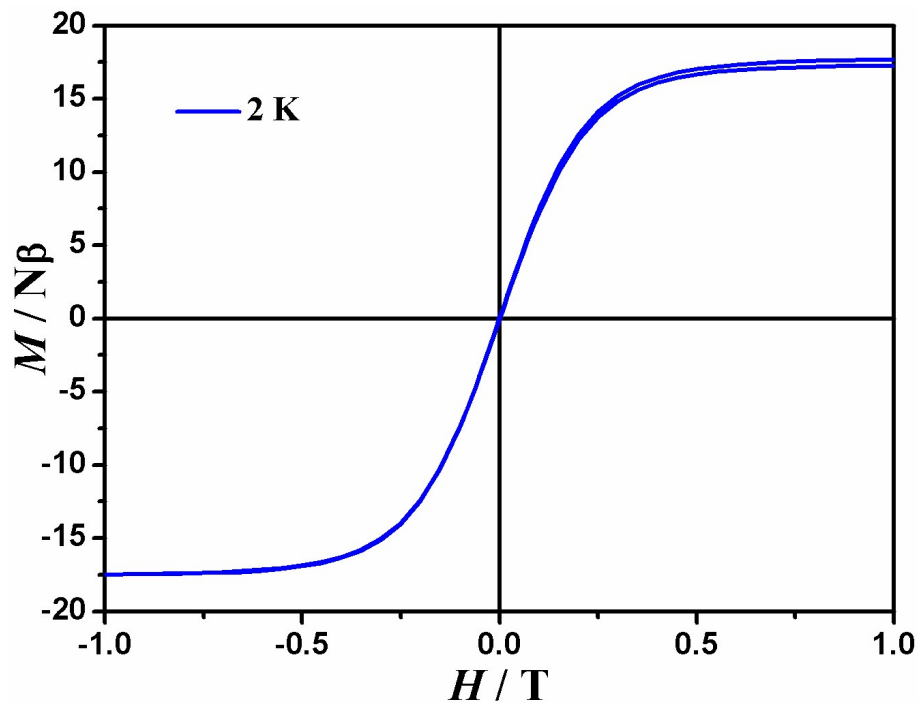
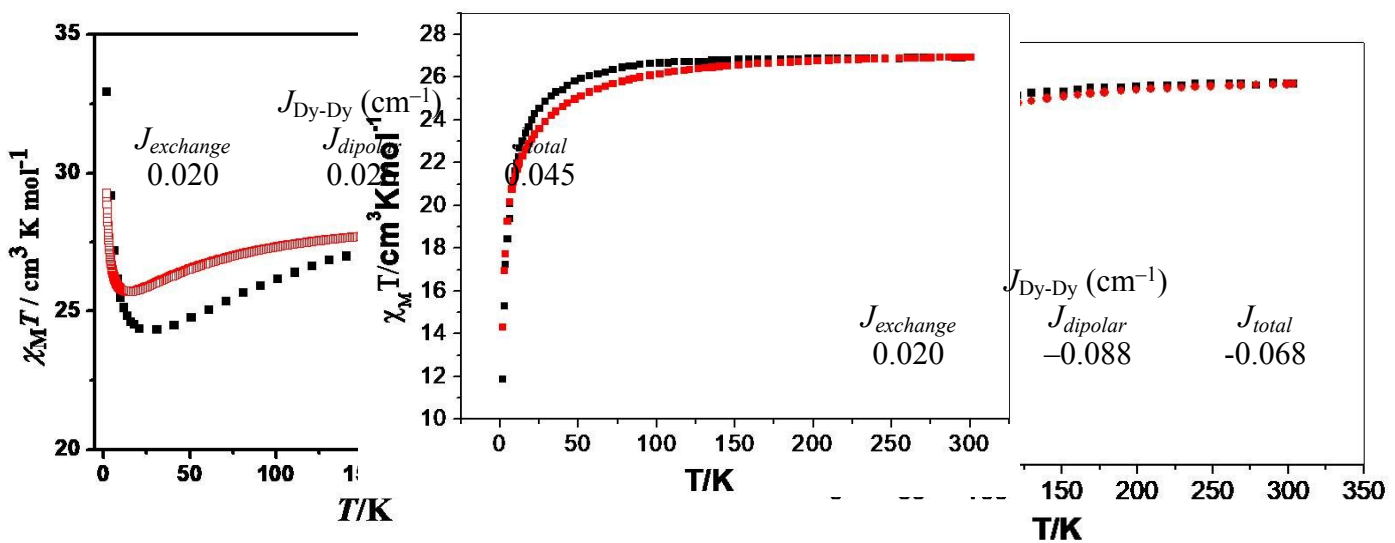


**Fig. S5.** Hysteresis loop measurement for **2** at 2 K.



$$\begin{array}{lll}
 J_{\text{exchange}} & J_{\text{Dy-Dy}} (\text{cm}^{-1}) & J_{\text{total}} \\
 0.015 & -0.099 & -0.074 \\
 \end{array}$$

**Fig. S6.** Best fit for  $\chi_M T$  vs  $T$  obtained using POLY\_ANISO for complexes **2–4**. Black color indicates experimental plot whereas red color indicates computed plot using POLY\_ANISO.

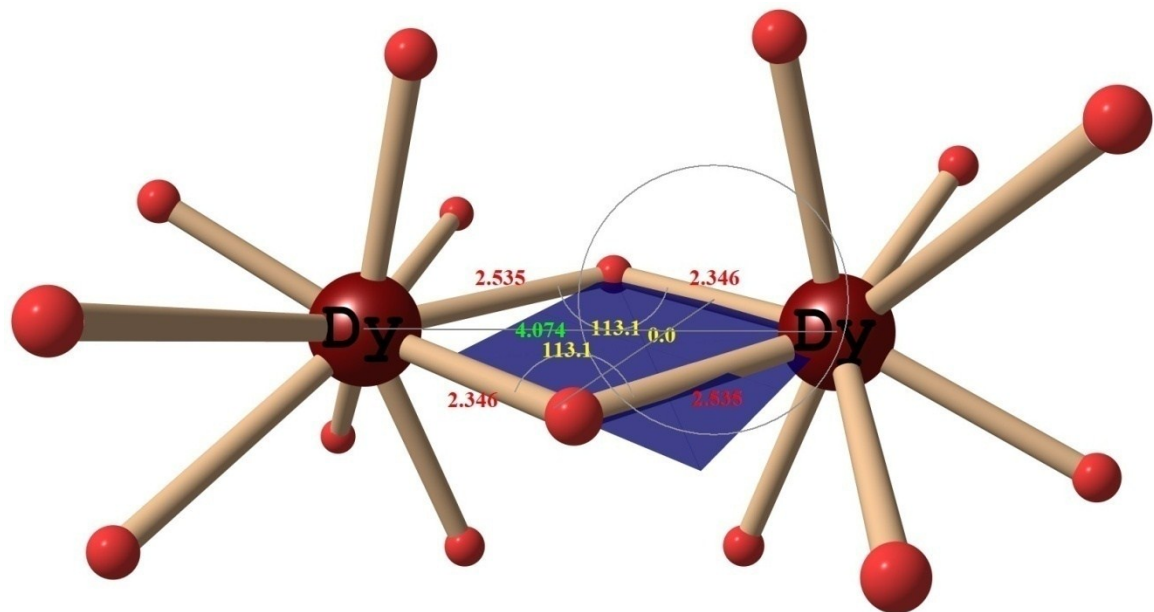
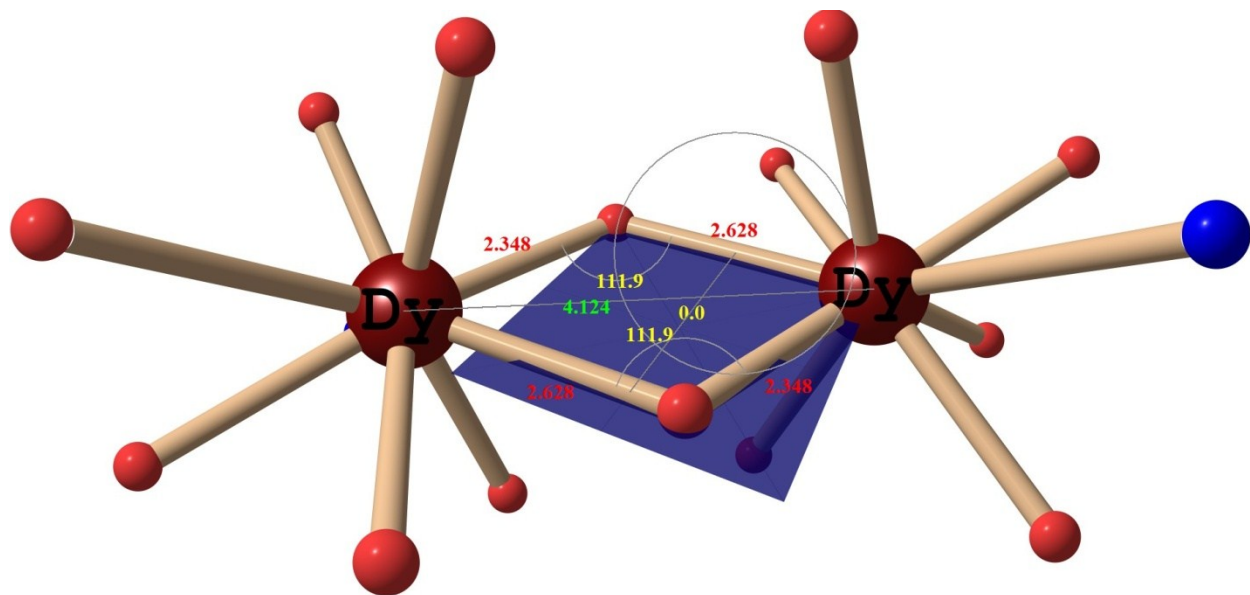
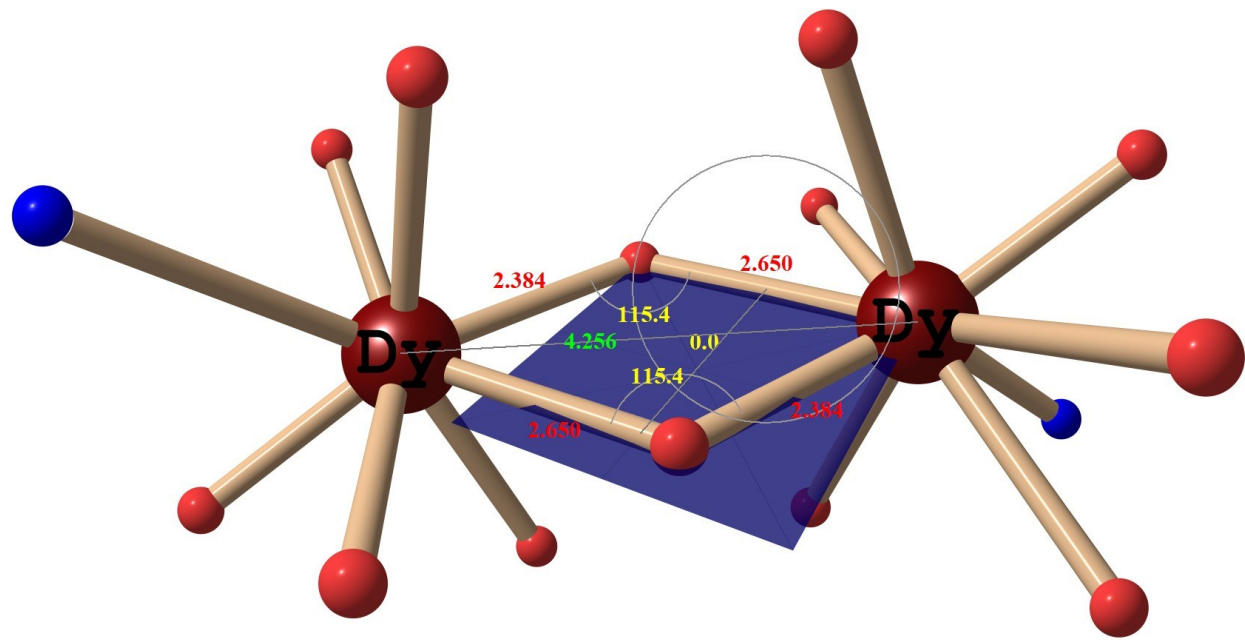


**Fig. S7.** Important structural parameters for complexes **2-4** (upper, middle and lower respectively), which are expected to control magnetic exchange interaction. Previous study (T. Rajeshkumar and G. Rajaraman et al. *Polyhedron*, 2013, **52**, 1299) suggests smaller avg. Ln–O (between 2.2 Å to 2.6 Å) bond distance and larger avg. Ln–O–Ln bond angle (between 100° to 120°) yielding larger ferromagnetic interaction. The avg. Ln–O bond distance and avg. Ln–O–Ln bond angle for complexes **2** (2.517 Å and 115.4°), **3** (2.488 Å and 111.9°) and **4** (2.441 Å and 113.1°) suggest same magnitude of ferromagnetic exchange coupling constant ( $J_{\text{exchange}} \sim 0.15$  to  $0.20 \text{ cm}^{-1}$ ).

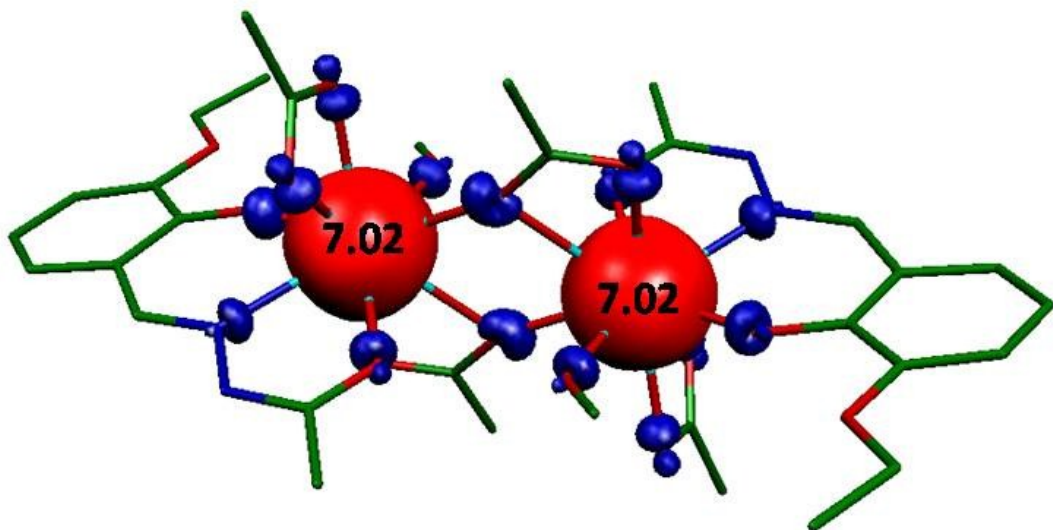


**Fig. S8.** DFT computed spin density plot for complex **1**. Very small spin density on the bridging atoms (< 0.005) suggest very small magnitude of magnetic coupling between both Gd<sup>III</sup> ions. The isodensity surface shown corresponds to a value of 0.001 e<sup>-</sup>/bohr<sup>3</sup>.

**Table S1.** The geometries of the hydrogen bonds (distances in Å and angles are in °) in **1** and **2**.

D–H···A	D···A		H···A		D–H···A	
	<b>1</b>	<b>2</b>	<b>1</b>	<b>2</b>	<b>1</b>	<b>2</b>
N2–H2A···O6E	2.724	2.734	1.924	1.932	175.88	172.35
C12–H12B···O5F	3.523	3.553	2.624	2.707	156.18	147.33
O4–H4A···O2D	2.741	2.729	1.958	1.940	168.55	175.01

**Table S2.** Relaxation fitting parameters from the least-square fitting of the Cole-Cole plots according to the generalized Debye model for **2**.

Temperature / K	$\chi_S / \text{cm}^3 \text{mol}^{-1} \text{K}$	$\chi_T / \text{cm}^3 \text{mol}^{-1} \text{K}$	$\tau / \text{s}$	$\alpha$
7	0.57008	6.54612	0.00438129	0.0523162
8	0.50639	5.63797	0.00216183	0.037723
9	0.46053	4.96953	0.00115581	0.0298736
10	0.42184	4.41256	6.48365E-4	0.0257698
11	0.41492	4.02072	3.79112E-4	0.0251362
12	0.42011	3.65994	2.11113E-4	0.0254141

**Table S3.** Comparison of bond lengths (in Å) around Dy<sup>III</sup>centre in compounds **2** and **3**<sup>15</sup>

Compound <b>2</b>	Compound <b>3</b>	Difference ( $\Delta$ )		
Dy1–O1	2.193	Dy1–O2	2.254	0.061
Dy1–O2	2.405	Dy1–O1	2.380	0.025
Dy1–N1	2.530	Dy1–N3	2.538	0.008
Dy1–O4	2.374	Dy1–O7	2.378	0.004
Dy1–O5	2.436	Dy1–O4	2.419	0.017
Dy1–O6	2.452	Dy1–O3	2.434	0.018
Dy1–O7	2.423	Dy1–O5	2.411	0.012
Dy1–O8	2.384	Dy1–O6A	2.348	0.036
Dy1–O8D	2.650	Dy1–O6	2.628	0.022

**Table S4.** Comparison of bond angles (in °) around Dy<sup>III</sup>centre in compounds **2** and **3**<sup>15</sup>

Compound 2		Compound 3		Difference ( $\Delta$ )
O1–Dy1–N1	70.26(12)	O1–Dy1–N3	63.47	6.79
O1–Dy1–O2	133.09(11)	O1–Dy1–O2	129.69	3.4
O1–Dy1–O4	79.37(11)	O1–Dy1–O7	76.35	3.02
O1–Dy1–O5	97.53(13)	O1–Dy1–O4	94.42	3.11
O1–Dy1–O6	77.02(13)	O1–Dy1–O3	73.06	3.96
O1–Dy1–O7	81.50(13)	O1–Dy1–O6A	81.72	0.22
O1–Dy1–O8	148.03(11)	O1–Dy1–O5	149.61	1.58
O1–Dy1–O8D	124.77(12)	O1–Dy1–O6	139.84	15.07
N1–Dy1–O2	64.13(11)	N3–Dy1–O2	69.07	4.94
N1–Dy1–O4	147.77(12)	N3–Dy1–O7	138.04	9.73
N1–Dy1–O5	68.73(12)	N3–Dy1–O4	70.12	1.39
N1–Dy1–O6	106.52(11)	N3–Dy1–O3	103.12	3.4
N1–Dy1–O7	81.11(12)	N3–Dy1–O6A	87.06	5.95
N1–Dy1–O8	136.42(11)	N3–Dy1–O5	134.13	2.29
N1–Dy1–O8D	118.14(10)	N3–Dy1–O6	136.49	18.35
O2–Dy1–O4	140.99(10)	O2–Dy1–O7	140.74	0.25
O2–Dy1–O5	76.18(11)	O2–Dy1–O4	84.32	8.14
O2–Dy1–O6	125.63(11)	O2–Dy1–O3	135.51	9.88
O2–Dy1–O7	81.32(12)	O2–Dy1–O6A	80.12	1.2
O2–Dy1–O8	78.15(10)	O2–Dy1–O5	78.49	0.34
O2–Dy1–O8D	71.67(10)	O2–Dy1–O6	71.75	0.08
O4–Dy1–O5	127.44(13)	O7–Dy1–O4	127.19	0.25
O4–Dy1–O6	75.91(13)	O7–Dy1–O3	74.59	1.32
O4–Dy1–O7	84.06(14)	O7–Dy1–O6A	75.25	8.81
O4–Dy1–O8	75.80(11)	O7–Dy1–O5	87.17	11.37
O4–Dy1–O8D	71.10(11)	O7–Dy1–O6	70.88	0.22
O5–Dy1–O6	52.81(11)	O4–Dy1–O3	53.32	0.51
O5–Dy1–O7	148.00(12)	O4–Dy1–O6A	155.87	7.87
O5–Dy1–O8	82.22(11)	O4–Dy1–O5	75.31	6.91
O5–Dy1–O8D	137.46(11)	O4–Dy1–O6	123.81	13.65
O6–Dy1–O7	152.88(12)	O3–Dy1–O6A	144.34	8.54
O6–Dy1–O8	77.65(12)	O3–Dy1–O5	78.05	0.4
O6–Dy1–O8D	134.51(10)	O3–Dy1–O6	118.03	16.48
O7–Dy1–O8	115.17(11)	O6A–Dy1–O5	118.87	3.7
O7–Dy1–O8D	50.53(10)	O6–Dy1–O6A	68.13	17.6
O8–Dy1–O8D	64.64(12)	O5–Dy1–O6	50.84	13.8
Dy1–O8–Dy1D	115.36(12)	Dy1–O6–Dy1A	111.87	3.49

**Table S5.** Comparison of bond lengths (in Å) around Gd<sup>III</sup> centre in compounds **1** and **7<sup>15</sup>**

Compound 1		Compound 7		Difference ( $\Delta$ )
Gd1–O1	2.224	Gd1–O2	2.246	0.022
Gd1–O2	2.427	Gd1–O1	2.399	0.028
Gd1–N1	2.547	Gd1–N3	2.553	0.006
Gd1–O4	2.404	Gd1–O7	2.385	0.019
Gd1–O5	2.458	Gd1–O4	2.415	0.043
Gd1–O6	2.468	Gd1–O3	2.420	0.048
Gd1–O7	2.452	Gd1–O5	2.444	0.008
Gd1–O8	2.621	Gd1–O6	2.602	0.019
Gd1–O8D	2.422	Gd1–O6A	2.340	0.082

**Table S6.** Comparison of bond angles (in  $^{\circ}$ ) around Gd<sup>III</sup> centre in compounds **1** and **7**<sup>15</sup>

Compound 1		Compound 7		Difference ( $\Delta$ )
O1–Gd1–N1	69.92(11)	O1–Gd1–N3	62.64	7.28
O1–Gd1–O2	132.36(11)	O1–Gd1–O2	128.32	4.04
O1–Gd1–O4	79.57(11)	O1–Gd1–O7	77.07	2.5
O1–Gd1–O5	96.89(12)	O1–Gd1–O4	92.94	3.95
O1–Gd1–O6	77.11(13)	O1–Gd1–O3	72.81	4.3
O1–Gd1–O7	81.23(12)	O1–Gd1–O6A	82.58	1.35
O1–Gd1–O8D	148.15(12)	O1–Gd1–O5	148.88	0.73
O1–Gd1–O8	124.84(11)	O1–Gd1–O6	141.16	16.32
N1–Gd1–O2	63.53(11)	N3–Gd1–O2	68.37	4.84
N1–Gd1–O4	147.58(11)	N3–Gd1–O7	138.12	9.46
N1–Gd1–O5	68.96(12)	N3–Gd1–O4	68.69	0.27
N1–Gd1–O6	106.72(12)	N3–Gd1–O3	102.58	4.14
N1–Gd1–O7	80.60(12)	N3–Gd1–O6A	88.36	7.76
N1–Gd1–O8D	136.45(11)	N3–Gd1–O5	133.08	3.37
N1–Gd1–O8	117.68(11)	N3–Gd1–O6	137.12	19.44
O2–Gd1–O4	141.85(10)	O2–Gd1–O7	141.9	0.05
O2–Gd1–O5	76.01(11)	O2–Gd1–O4	83.8	7.79
O2–Gd1–O6	125.15(12)	O2–Gd1–O3	135.42	10.27
O2–Gd1–O7	81.80(12)	O2–Gd1–O6A	80.57	1.23
O2–Gd1–O8D	78.57(10)	O2–Gd1–O5	79.52	0.95
O2–Gd1–O8	72.28(10)	O2–Gd1–O6	72.63	0.35
O4–Gd1–O5	127.13(14)	O7–Gd1–O4	127.28	0.15
O4–Gd1–O6	75.85(13)	O7–Gd1–O3	74.13	1.72
O4–Gd1–O7	84.24(14)	O7–Gd1–O6A	74.99	9.25
O4–Gd1–O8D	75.97(11)	O7–Gd1–O5	87.71	11.74
O4–Gd1–O8	71.42(11)	O7–Gd1–O6	71.3	0.12
O5–Gd1–O6	52.42(12)	O4–Gd1–O3	53.71	1.29
O5–Gd1–O7	147.97(13)	O4–Gd1–O6A	155.83	7.86
O5–Gd1–O8D	82.23(11)	O4–Gd1–O5	74.8	7.43
O5–Gd1–O8	138.00(11)	O4–Gd1–O6	124.11	13.89
O6–Gd1–O7	152.80(12)	O3–Gd1–O6A	143.97	8.83
O6–Gd1–O8D	77.37(11)	O3–Gd1–O5	76.99	0.38
O6–Gd1–O8	134.81(11)	O3–Gd1–O6	117.71	17.1
O7–Gd1–O8D	115.82(11)	O6A–Gd1–O5	119.78	3.96
O7–Gd1–O8	50.65(10)	O6A–Gd1–O6	68.05	17.4
O8D–Gd1–O8	65.18(12)	O5–Gd1–O6	51.8	13.68
Gd1–O8–Gd1D	114.82(12)	Gd1–O6–Gd1A	111.95	2.87

## Computational Details

*Ab initio*CASSCF<sup>1</sup>+RASSI-SO<sup>2</sup>+SINGLE\_ANISO<sup>3,4</sup>calculations have been performed on all paramagnetic ions using the single crystal structure data in MOLCAS 8.0<sup>5-9</sup>suite by keeping the ion of interest (Dy<sup>III</sup>) as such and substituting the second paramagnetic ions with diamagnetic ions (La<sup>III</sup>/Sc<sup>III</sup>) without altering other parts. We have used C.ANO-RCC...3s2p.,O.ANO-RCC...3s2p1d.,H.ANO-RCC...2s.,Lu.ANO-RCC...7s6p4d2f1g.,Dy.ANO-RCC...8s7p5d3f2g1h.. basis sets for our *ab initio* calculations.<sup>10</sup>For our CASSCF calculations on single Dy<sup>III</sup> ion, we have used nine electrons in seven active 4f orbitals. Next, in the RASSI-SO step, 21 roots for sextet spin multiplicity has been considered.<sup>11</sup>The resultant spin-orbit multiplet has been further used to calculate local magnetic properties via SINGLE\_ANISO approach. The magnetic exchange interactions ( $J_s$ ) have been computed between all paramagnetic ions for all complexes by fitting *ab initio* POLY\_ANISO with the experimental data.<sup>12-14</sup>

**Table S7.** *Ab initio* computed g-tensors along with the energy and the angle for eightlowest KDs both Dy<sup>III</sup>centres in **2–4**.

Dy1 ( <b>2</b> ) KD	E cm <sup>-1</sup>	g <sub>xx</sub>	g <sub>yy</sub>	g <sub>zz</sub>	Angle (°)
1	0.0	0.042	0.065	19.788	
2	99.6	1.279	2.404	16.279	31.4
3	155.4	1.987	3.994	11.961	67.8
4	200.3	0.605	1.577	16.299	83.8
5	237.4	1.251	4.860	10.189	77.1
6	299.6	1.559	2.137	15.754	71.9
7	333.2	0.564	0.935	16.662	74.2
8	449.7	0.088	0.112	19.221	57.8

Dy2 ( <b>2</b> ) KD	E cm <sup>-1</sup>	g <sub>xx</sub>	g <sub>yy</sub>	g <sub>zz</sub>	Angle (°)
1	0.0	0.042	0.065	19.788	
2	99.6	1.280	2.405	16.278	31.4
3	155.3	1.985	3.993	11.960	67.8
4	200.2	0.606	1.575	16.303	83.8
5	237.4	1.251	4.862	10.186	77.1
6	299.5	1.559	2.138	15.754	71.9
7	333.1	0.564	0.935	16.661	74.2
8	449.6	0.0879	0.112	19.222	57.8

Dy1 ( <b>3</b> ) KD	E cm <sup>-1</sup>	g <sub>xx</sub>	g <sub>yy</sub>	g <sub>zz</sub>	Angle (°)
1	0.0	0.005	0.016	19.870	
2	141.6	0.156	0.452	17.208	23.7
3	197.0	2.615	5.341	12.547	73.1
4	228.1	1.557	2.631	11.746	118.1
5	284.8	3.655	6.320	9.275	100.6
6	339.5	0.032	0.269	18.122	86.9
7	395.7	0.470	0.844	16.820	110.4
8	585.3	0.041	0.068	19.570	85.3

Dy2 ( <b>3</b> ) KD	E cm <sup>-1</sup>	g <sub>xx</sub>	g <sub>yy</sub>	g <sub>zz</sub>	Angle (°)
1	0.0	0.005	0.016	19.870	
2	141.6	0.155	0.451	17.225	23.7
3	197.0	2.608	5.348	12.504	73.2
4	228.1	1.546	2.633	11.718	118.3
5	284.8	3.656	6.310	9.255	100.6
6	339.5	0.031	0.267	18.082	86.9
7	395.7	0.470	0.841	16.794	110.5
8	585.3	0.040	0.068	19.543	85.3

Dy1 ( <b>4</b> ) KD	E cm <sup>-1</sup>	g <sub>xx</sub>	g <sub>yy</sub>	g <sub>zz</sub>	Angle (°)
1	0.0	0.096	0.151	19.282	
2	71.0	1.607	3.230	14.495	9.5
3	103.0	1.753	5.251	10.931	61.9
4	149.7	9.634	6.333	1.030	50.9
5	200.2	2.037	3.968	13.355	92.5
6	241.0	0.171	1.141	17.047	101.1
7	293.3	0.533	1.048	15.360	76.6
8	422.2	0.032	0.046	19.347	89.6

Dy2 ( <b>4</b> ) KD	E cm <sup>-1</sup>	g <sub>xx</sub>	g <sub>yy</sub>	g <sub>zz</sub>	Angle (°)
1	0.0	0.084	0.200	19.253	
2	65.5	0.810	1.211	15.477	12.7
3	116.6	1.619	3.809	12.944	122.9
4	170.3	0.130	5.013	10.469	39.3
5	230.8	9.250	5.504	0.710	123.2
6	264.0	0.690	5.496	11.075	89.7
7	305.6	1.387	3.907	11.773	84.5
8	334.0	1.235	3.201	16.932	99.4

**Table S8.** *Ab initio* SINGLE\_ANISO computed crystal field parameters for complexes **2**, **3** and **4**. The non-axial term ( $B_k^q$ , where  $q \neq 0$  and  $k = 2, 4$ , and  $6$ ) to the axial term ( $B_k^q$ , where  $q = 0$  and  $k = 2, 4$ , and  $6$ ) ratio should be smaller for lesser operational QTM and larger  $U_{cal}$  value.

Here, k - the rank of the ITO, = 2, 4, 6, 8, 10, 12.

q - the component of the ITO, = -k, -k+1, ... 0, 1, ... k;

$K_m^n$  are proportionality coefficients between the ESO and operators.

k	q	$K_m^n$	Complexes							
			Dy1 (2)		Dy2(2)		Dy1 (3)		Dy2(3)	Dy1 (4)
2	-2	1.5	0.12	0.12	-2.52	-2.53	1.19	0.20		
2	-1	6.0	-1.53	-1.53	0.96	0.96	0.27	0.09		
2	0	1.0	-1.29	-1.29	-2.05	-2.05	-1.45	-1.43		
2	1	6.0	-2.42	-2.42	0.37	0.35	0.39	-1.23		
2	2	1.5	1.59	1.59	0.87	0.86	1.53	1.00		

**Table S9.** POLY\_ANISO fitted  $J_{\text{Dy-Dy}}$  value for complexes **2–4**.

Complex	$J_{\text{Dy-Dy}} (\text{cm}^{-1})$		
	$J_{\text{exchange}}$	$J_{\text{dipolar}}$	$J_{\text{total}}$
<b>2</b>	0.020	0.025	0.045
<b>3</b>	0.020	-0.088	-0.068
<b>4</b>	0.015	-0.099	-0.074

**Table S10.** Continuous Shape measures calculation for complexes **2–4**.

EP-9	1 D9h	Enneagon
OPY-9	2 C8v	Octagonal pyramid
HBPY-9	3 D7h	Heptagonal bipyramid
JTC-9	4 C3v	Johnson triangular cupola J3
JCCU-9	5 C4v	Capped cube J8
CCU-9	6 C4v	Spherical-relaxed capped cube
JCSAPR-9	7 C4v	Capped square antiprism J10
CSAPR-9	8 C4v	Spherical capped square antiprism
JTCTPR-9	9 D3h	Tricapped trigonal prism J51
TCTPR-9	10 D3h	Spherical tricapped trigonal prism
JTDIC-9	11 C3v	Tridiminished icosahedron J63
HH-9	12 C2v	Hula-hoop
MFF-9	13 Cs	Muffin

Structure [ML9]	EP-9	OPY-9	HBPY-9	JTC-9	JCCU-9	CCU-9	JCSAPR-9	CSAPR-9	JTCTPR-9	TCTPR-9	JTDIC-9	HH-9	MFF-9	Ref.
Dy1	32.797	20.984	16.835	13.893	9.828	8.939	2.168	<b>1.787</b>	2.962	2.895	12.421	9.772	1.900	This work
Dy2	32.797	20.984	16.835	13.893	9.828	8.939	2.168	<b>1.787</b>	2.962	2.895	12.421	9.772	1.900	This work
Dy1	34.490	23.385	17.863	13.422	8.177	7.789	2.245	<b>1.918</b>	3.181	2.660	11.563	10.358	<b>1.849</b>	15
Dy2	34.490	23.385	17.863	13.422	8.177	7.789	2.245	<b>1.918</b>	3.181	2.660	11.563	10.358	<b>1.849</b>	15
Dy1	33.973	22.532	18.164	14.987	10.377	8.793	3.136	<b>2.102</b>	4.645	2.825	10.916	9.211	<b>1.932</b>	16
Dy2	33.974	22.532	18.164	14.987	10.377	8.793	3.136	<b>2.102</b>	4.644	2.825	10.916	9.211	<b>1.932</b>	16

## References:

- 1 B.Swerts, L. F.Chibotaru, R.Lindh, L.Seijo, Z.Barandiaran, S.Clima, K.Pierloot and M. F. A.Hendrickx, *J. Chem.Theory Comput.*,2008,**4**, 586.
- 2 P. Å.Malmqvist, B. O.Roos and B.Schimmelpfennig, *Chem. Phys. Lett.*,2002,**357**, 230.
- 3 L. F.Chibotaru and L.Ungur, *J. Chem. Phys.*,2012,**137**, 064112.
- 4 L. F.Chibotaru, A.Ceulemans and H.Bolvin, *Phys. Rev. Lett.*2008,**101**, 033003.
- 5 F.Aquilante,J.Autschbach, R. K.Carlson, L. F.Chibotaru, M. G.Delcey, L.De Vico, G. I. Fdez, N.Ferré, L. M.Frutos, L.Gagliardi, M.Garavelli, A.Giussani, C. E.Hoyer, M. G.Li, H.Lischka, D.Ma, P.-Å.Malmqvist, T.Müller, A.Nenov, M.Olivucci, T. B.Pedersen, D.Peng, F.Plasser, B.Pritchard,M. Reiher, I.Rivalta,I. Schapiro, J.Segarra-Martí, M.Stenrup, D. G.Truhlar, L.Ungur, A.Valentini, S.Vancoillie, V.Veryazov, V. P.Vysotskiy, O.Weingart, F. Zapata andR. Lindh, *J. Comput. Chem.*,2015,**37**, 506.
- 6 F.Aquilante, L.De Vico, N.Ferré, G.Ghigo, P.-Å.Malmqvist, P.Neogrády, T. B.Pedersen, M.Pitoňák, M.Reiher, B. O.Roos, L.Serrano-Andrés, M.Urbán, V.Veryazov and R.Lindh, MOLCAS 7: The Next Generation.,*J. Comput. Chem.*,2010,**31**, 224.
- 7 J. A.Duncan, MOLCAS 7.2.,*J. Am. Chem. Soc.*, 2009,**131**, 2416.
- 8 V.Veryazov, P. O.Widmark, L.Serrano-Andrés, R.Lindh and B. O.Roos, *Int. J. Quantum Chem.*,2004,**100**, 626.
- 9 G.Karlström, R.Lindh, P.-Å.Malmqvist,B. O.Roos, U.Ryde, V.Veryazov, P.-O.Widmark, M.Cossi, B.Schimmelpfennig,P.Neogrady and L.Seijo, *Comput. Mater. Sci.*2003,**28**, 222.
- 10 B. O.Roos, R.Lindh, P.-Å.Malmqvist, V.Veryazov, P.-O.Widmark and A. C.Borin,*J. Physi.Chem. A*,2008,**112**, 11431.
- 11 K.Bernot, J.Luzon, L.Bogani, M.Etienne, C.Sangregorio, M.Shanmugam, A.Caneschi, R.Sessoli and D.Gatteschi, *J. Am. Chem. Soc.*,2009,**131**, 5573.
- 12 L.Chibotaru, L.Ungur and A.Soncini, *Angew. Chem., Int. Ed.*,2008,**47**, 4126.
- 13 L.Ungur,W.Van den Heuvel and L. F.Chibotaru, *New J. Chem.*2009,**33**, 1224.
- 14 L. F.Chibotaru, L.Ungur, C.Aronica, H.Elmoll,G.Pilet and D.Luneau, *J. Am. Chem. Soc.*,2008,**130**, 12445.
- 15 H. Zhang, S.-Y. Lin, S. Xue, C. Wanga and J. Tang, *DaltonTrans.*, 2014, **43**, 6262.
- 16 B. Joarder, A. K. Chaudhari, G. Rogezb and S. K. Ghosh, *DaltonTrans.*, 2012, **41**, 7695.